



Assessing climate change impacts on water resources in the Benue River Basin, Northern Cameroon

Rodric M. Nonki¹ · André Lenouo² · Christopher J. Lennard³ · Clément Tchawoua⁴

Received: 28 November 2018 / Accepted: 23 September 2019 / Published online: 8 October 2019
© Springer-Verlag GmbH Germany, part of Springer Nature 2019

Abstract

The Benue River Basin (BRB) is a major tributary of the Niger River Basin (NRB) and the second-largest river in Cameroon. It serves many water resource functions including irrigation, hydroelectricity production and navigation. Previous research has indicated that recent climate change (CC) has had significant impacts on local and regional hydrological regimes of this watershed. In this study, CC scenarios were integrated with a hydrological model to evaluate the influence of CC on water resources in the BRB. Historical and projected scenarios of dynamically downscaled temperature and precipitation from the REMO regional climate model (RCM) forced by the boundary conditions data of the Europe-wide Consortium Earth System Model (EC-ESM) and the Max Planck Institute-Earth System Model (MPI-ESM) general circulation models (GCMs) were used. The historical runs of the REMO simulations were first evaluated after which downscaled temperature and precipitation data were used as input for the HBV-Light hydrological model to simulate water balance components. The mean climate and hydrological variables for the historical (1981–2005) and the two future periods (2041–2065 and 2071–2095) were compared to assess the potential impact of CC on water resources in the middle and late twenty-first century under three greenhouse gases (GHGs) concentration scenarios, the Representative Concentration Pathways (RCPs) 2.6, 4.5 and 8.5. Our results show that (a) the HBV-Light hydrological model could effectively simulate the streamflow change in the BRB; (b) annual precipitation will decrease between 1 and 10% while both annual temperature and potential evapotranspiration (PET) will increase between 8–18 and 6–30%, respectively, under both scenarios, models and future periods; c) the combination of reduced precipitation and increase of PET results in a significant decrease in streamflow in the BRB (up to 51%) and this will move the basin to a much drier environmental state. Therefore, CC adaptation strategies and future development planning in this region must consider these important decreases of discharge.

Keywords Climate change · Water resources · REMO model · HBV-Light hydrological model · Dynamical downscaling · Benue River Basin

Electronic supplementary material The online version of this article (<https://doi.org/10.1007/s12665-019-8614-4>) contains supplementary material, which is available to authorized users.

✉ Rodric M. Nonki
norome31@yahoo.fr

- ¹ Laboratory for Environmental Modeling and Atmospheric Physics (LEMAP), Department of Physics, Faculty of Sciences, University of Yaounde I, Yaoundé, Cameroon
- ² Department of Physics, Faculty of Science, University of Douala, Douala, Cameroon
- ³ Climate System Analysis Group, University of Cape Town, Cape Town, South Africa
- ⁴ Laboratory of Mechanics, Department of Physics, Faculty of Sciences, University of Yaounde I, Yaoundé, Cameroon

Introduction

Cameroon contributes significantly to the economy of Central Africa (CA), its water resources being a major source of this importance. However, within Cameroon, water is also recognized as the most important impediment for socio-economic development because more than 70% of the population practices rainfed agriculture, which occupies about 95% of the land use (Molua and Lambi 2007). Other activities are also dependent on water resources: hydroelectricity production represents more than 95% of electricity in Cameroon. Additionally, Cameroon has the second-highest hydropower potential in CA after the Democratic Republic of Congo. However, in Cameroon, water resources are unequally distributed between the northern and southern parts. The

southern part (up to 6°N) experiences a wet sub-tropical climate with annual precipitation ranging between 1500 and 4000 mm. In the northern part, the climate is semi-arid to arid Sahelian with annual rainfall less than 400 mm in the northernmost (13°N) part (Kamga 2001) and where many rivers dry up a few months after the rainy season. The Benue River Basin (BRB), the second-largest river in Cameroon, is a perennial river in Northern Cameroon and holds huge water resource potential including hydropower, irrigation, and navigation due to the construction of the Lagdo dam and its hydropower plant in 1982.

Northern Cameroon experiences water-related disasters such as floods (Sighomnou et al. 2013) and droughts (Molua and Lambi 2006; Gao et al. 2011). Additionally, water shortages in northern Cameroon are also the result of population growth, which naturally increases the water demand, poor water resources management (WRM) and changing environmental conditions (Cheo et al. 2013). Recent studies (Fotso-Nguemo et al. 2017a, b; Mba et al. 2018; Sonkoué et al. 2018; Tamoffo et al. 2019b) have shown evidence of decreased precipitation and increased temperature over the Sahelian region. According to the Fifth Assessment Report (AR5) of the Intergovernmental Panel on Climate Change (IPCC 2013), the risk of water disasters such as flood, drought and water shortage will be exacerbated due to CC. Many authors show that water discharge and quality are strongly controlled by rainfall events (Khan et al. 2015, 2016a, b; Sakho et al. 2017); therefore, under CC proper spatio-temporal water resource planning is essential to develop robust WRM solutions and development projects in the country. It is also important to build tools that can help decision-makers better manage regional water resources (planning, design, operation and management of water resources systems).

One way to study the impacts of CC on water resources is to force hydrological models with input data (temperature and precipitation) that come from general circulation models (GCMs) (Kamga 2001; Obeysekera et al. 2011; Sahoo et al. 2011; Tshimanga and Hughes 2012). According to Chou et al. (2014), CC impact assessment at the regional scale needs higher resolution spatial data. As impacts and vulnerabilities of a given region are linked to regional and local forcings, GCMs with a coarse horizontal grid resolution do not capture these local and regional effects (Deb et al. 2015). It is therefore important to downscale the input variables for a hydrological model to the spatial and temporal scales that resolve the local climate features and are needed by the hydrological model. In this context, the Coordinated Regional Climate Downscaling EXperiment project (CORDEX; Giorgi et al. (2009); <http://www.cordex.org>), sponsored by the World Climate Research Program (WCRP; <http://www.wcrp-climate.org/>), has produced many down-scaled climate data for Africa derived from several regional

climate models (RCMs) that have downscaled many GCMs. The data derive from a set of dynamically downscaled models, forced by GCMs from phase 5 of the Coupled Model Intercomparison Project (CMIP5). Downscaled climate data have been used to analyze the impact of climate change on water resources globally (El-Khoury et al. 2015; Leta et al. 2016; Meng et al. 2016; Bajracharya et al. 2018; Nilawar and Waikar 2018; Saïdi et al. 2018; Mohammadzadeh et al. 2019; Sada et al. 2019; Xu et al. 2019) and over West and Central Africa (Cornelissen et al. 2013; Bossa et al. 2014; Aich et al. 2014, 2016; Roudier et al. 2014; Mbaye et al. 2015; Yira et al. 2017; Aloysius and Saiers 2017; Alamou et al. 2017; Oyerinde et al. 2017; Coulibaly et al. 2018; Stanzel et al. 2018) by driving hydrological models with down-scaled precipitation and temperature data.

Although downscaled climate data have been used to drive hydrological models in other regions in Africa (e.g., Trambly et al. 2013; Li et al. 2015), to date, no study has assessed the impact of CC on water resources over this important watershed by using downscaled precipitation and temperature data. Existing studies were based on GCM data (Kamga 2001; Sighomnou 2004). In this context, our research aims to evaluate the impact of CC on water resources in the BRB using dynamically downscaled precipitation and temperature data from the REMO RCM to drive the HBV-Light hydrological model. The specific objectives of this study are to: (1) evaluate the performance of the HBV-Light hydrological model to simulate streamflow in the BRB; (2) evaluate the ability of REMO model to simulate present-day climate over the BRB; and (3) evaluate the potential impact of CC on water resources in the BRB. We do this by comparing the mean climate and hydrological variables for the historical (1981–2005) and the two future periods (2041–2065 and 2071–2095) under three greenhouse gases (GHGs) concentration scenarios, the Representative Concentration Pathways (RCPs) 2.6, 4.5 and 8.5. This paper is divided into four sections. After the introduction, the materials and methods are presented in the second section. The third section is devoted to presenting and discussing the results, while the main findings and conclusion are presented in the fourth section.

Materials and methods

Study area

The study area is the BRB, located in the Northern Cameroon between latitudes 7°N and 11°N and longitudes 12°E and 16°E (Fig. 1). It is part of the Lower Niger River Basin (NRB) and considered as the main tributary of the NRB (Oguntunde and Abiodun 2013). The BRB has its source in the Adamawa plateau, from where it flows toward the west

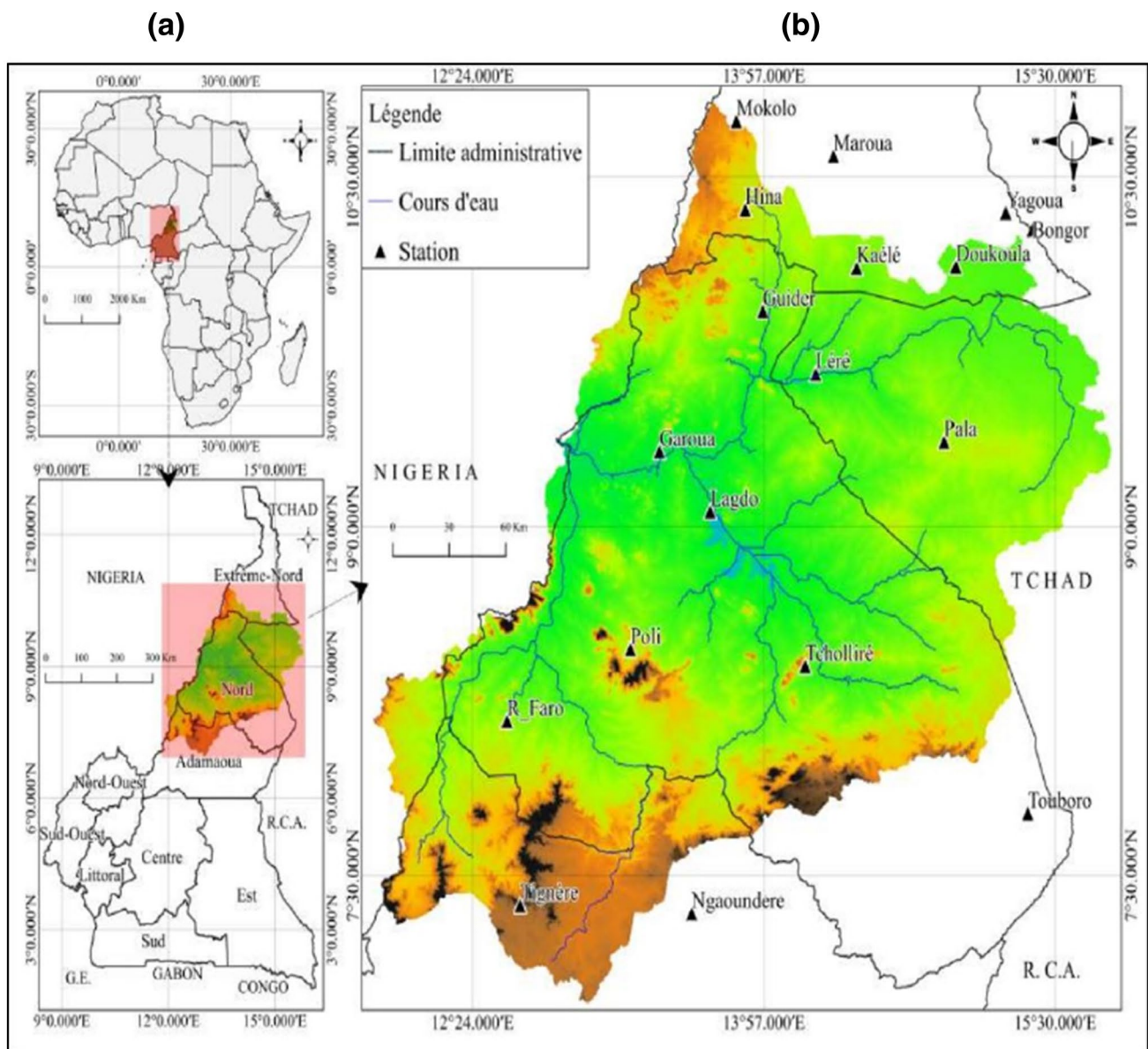


Fig. 1 Study area: basin localization (left), basin drainage area (right)

and crosses the city of Garoua and Lagdo Reservoir, into Nigeria South of the Mandara Mountains (Chisholm 1911). It is characterized by Savanna vegetation and elevations vary from 220 to 2260 m with the highland of Adamawa Plateau located in the southern part of the watershed (see Fig. S1). The BRB holds huge potentials for water resources, including hydropower, irrigation and navigation. It is therefore important for the entire northern Cameroon and the neighboring areas.

The BRB is located in the transition zone between the tropical/equatorial climate in the center and south of Cameroon and the Sahelian climate in the far north and enjoys a tropical humid climate (Sudanese climate). Seasonally, the

dry season stretches from November to April and the rainy season from May to October. It is a unimodal rainfall region (maximum in August) with annual rainfall ranging from 600 to 1500 mm (Molua and Lambi 2006; Cheo et al. 2013). Daily mean temperatures in the dry and rainy seasons range from 25.8 to 33 °C and 25.5 to 30.9 °C, respectively. Daily mean relative humidity ranges from 19.8 to 82.6% with an annual average of 51.2% (see Table 1).

Table 1 Long-term mean monthly temperature (T), precipitation (P), relative humidity (RH), day length sunshine (n) and Penman PET during the period (1979–2004) in Garoua region

Months	J	F	M	A	M	J	J	A	S	O	N	D	Annual
T (°C)	25.8	28.5	32.2	33.1	30.9	28.2	26.8	26.5	26.7	28.1	28.1	26	28.4
RH (%)	24.2	19.8	22.6	40.5	58.7	70.5	78	82.6	80.4	67.9	43.2	25.8	51.2
n (h)	2	8	2	6	3	0	4	6	4	4	8	8	5.4
PET (mm/day)	4.7	5.6	6.8	7.4	6.3	5.3	4.6	4.3	4.4	5.0	5.1	4.6	5.4
P (mm/month)	0	0.2	4.6	43.3	104.1	134.9	178.2	206.4	160.7	78.9	3	1.1	915.4

Data used

Hydrometeorological data

Daily measured weather data (precipitation and mean temperature) from the National Meteorological Service of Cameroon (NMSC), recorded at the different weather stations located in the basin and the neighboring areas, was used in this study. Rainfall data of some of those stations have been used to calibrate the Yates hydrological model in BRB (Kamga 2001), to divide Cameroon into different climatic zones (Penlap et al. 2004) and to investigate the onset, retreat and length of the rainy season and drought occurrence over Cameroon (Guenang and Mkankam 2012, 2014). The potential evapotranspiration (PET) was estimated using the Hamon (1961) method (refer to “Method to estimate Potential Evapotranspiration”).

The daily streamflow data measured at the available hydrometric stations (Buffle Noir, Garoua port and Riao) located in the basin were obtained from the Hydrosociences Montpellier database (Boyer et al. 2006, SIEREM, <http://hydrosociences.fr/sierem>). The streamflow data of Riao gauging station was used by Kamga (2001) to investigate the performance of Yates hydrological model in the BRB.

Climate model description and CORDEX simulation design

In this study, CORDEX precipitation and temperature data derived from REMO model, which has been used in other studies over the region (Fotso-Nguemo et al. 2017a, b; Vondou and Haensler 2017; Tamoffo et al. 2019b), were used to drive the hydrological model. Two GCMs (EC-Earth and MPI-ESM-LR) were downscaled by the REMO model over the CORDEX African domain (Giorgi et al. 2009) and are termed, respectively, REMO-EC and REMO-MPI. REMO is a hydrostatic and three-dimensional atmospheric model based on the “Europa-Model” system (Jacob 2001; Jacob et al. 2012; Teichmann et al. 2013). The model setup included a land surface scheme (Hagemann 2002), radiation scheme (Morcrette 1991) and a semi-Lagrangian advection scheme as well as the parameterization of sub-grid scale processes such as convection (Tiedtke 1989), cloud microphysics (Lohmann and

Roeckner 1996) and turbulent vertical diffusion (Louis 1979). The horizontal grid resolution was $0.44^\circ \times 0.44^\circ$ as specified by CORDEX. More information about the model physics and dynamics is available at the REMO website (<http://www.remo-rcm.de/>).

The historical experiments of the GCMs are downscaled for 1950–2005 in which observed (GHGs) concentrations were used. The GCM projections are downscaled from 2006 to 2100 and three RCP scenarios are considered, namely, RCP2.6 (Van Vuuren et al. 2011), RCP4.5 (Thomson et al. 2011) and RCP8.5 (Riahi et al. 2011).

To evaluate the capacity of REMO model to simulate the present climate (1983–2005), the output of REMO is compared to available observational and reanalysis datasets that include:

- Climate Research Unit data (CRU) version TS3.22 beginning in 1901 from the University of East Anglia that includes monthly precipitation and temperature at $0.5^\circ \times 0.5^\circ$ latitude–longitude resolution over land areas (Harris et al. 2014).
- The National Center for Environmental Prediction/National Center for Atmospheric Research (NCEP/NCAR) Reanalysis data (NCEP1) spans from 1948 to present and includes 6 hourly daily precipitation rates and 2-m temperature at $2.5^\circ \times 2.5^\circ$ spatial resolution (Kalnay et al. 1996).
- The National Center for Environmental Prediction (NCEP) of the Department of Energy (DOE) Atmospheric Model Intercomparison Project (AMIP-II) reanalysis data (NCEP2) spans from 1979 to 2016 and includes 6 hourly daily precipitation rate and 2-m temperature at a $2.5^\circ \times 2.5^\circ$ spatial resolution (Kanamitsu et al. 2002).
- The ERA-Interim Reanalysis data from the European Centre for Medium-Range Weather Forecasts (ECMWF) that includes daily precipitation and 2-m temperature at a $0.75^\circ \times 0.75^\circ$ spatial resolution (Dee et al. 2011).

To assess the performance of the REMO simulation against observational and reanalysis data, we compute the root mean square error (RMSE), the coefficient of determination (R^2) and the mean bias (MB) (Fotso-Nguemo et al. 2017b).

Table 2 HBV-Light model parameter definitions, units, reasonable ranges for variables which were calibrated in this study and calibrated value

Parameter	Definition	Units	Min value	Max value	Best value of calibrated parameter
Fc	Maximum value of soil moisture storage	mm	50	500	380.43
LP	Fraction of FC above which AET equals PET	–	0.3	1	0.69
β	Shape coefficient	–	1	6	3.16
K_0	Recession coefficient (upper box)	day ⁻¹	0.05	0.5	0.47
K_1	Recession coefficient (upper box)	day ⁻¹	0.01	0.3	0.10
K_2	Recession coefficient (lower box)	day ⁻¹	0.001	0.1	0.09
UZL	Threshold for surface flow	mm	0	100	94.09
PERC	Maximum rate of recharge between the upper and lower groundwater boxes	mm day ⁻¹	0	6	3.38
MAXBAS	Length of triangular weighting function in routing routine	day	1	5	1.94

Hydrological model

HBV-Light hydrological model concept

Initially developed in the Swedish Meteorological and Hydrological Institute (SMHI) by Bergstrom (1976), the HBV (Hydrologiska Byrans Vattenavdelning) model is a lumped and conceptual model for watershed which simulates discharges using rainfall, temperature and PET as input. The model consists of three main routines: snowmelt and snow cover routine, soil moisture and evaporation routine, runoff routine represented by two mains reservoirs. All these main hydrological processes in the HBV model are simplified by the model parameters (Table 2). More explanations of the model can be found in various works (Seibert 1999; Abebe et al. 2010; Aghakouchak and Habib 2010; Seibert and Vis 2012; Zelelew and Alfredsen 2013). The version of the model used in this study is the one developed by Seibert (2005) called HBV-Light. It provided an easy to use Windows software version of the model for research and education. The model used a “warming-up” period during the calibration.

Given that the watershed is snow free, the rainfall (P [mm]) is divided into water infiltration and surface runoff depending on the relation between the water content of the soil box (SM [mm]) and its largest value (FC [mm]). The second component, usually known as effective precipitation (P_{eff} [mm]), is given by Eq. 1:

$$P_{eff} = P \cdot \left(\frac{SM}{FC} \right)^\beta, \tag{1}$$

where a parameter β determines the relative contribution to runoff from a millimeter of rain at a given soil moisture deficit.

Actual evapotranspiration (AET) from the soil box equals to the PET if SM/FC is above LP [–], while a linear reduction is used when SM/FC is below LP (Eq. 2):

$$AET = PET \cdot \min\left(1, \frac{SM}{FC \cdot LP}\right), \tag{2}$$

where LP is a parameter that controls the shape of the reduction curve for PET.

Surface runoff is added to the upper groundwater box (SUZ [mm]) and streamflow from the groundwater boxes is computed as the sum of two or three linear outflow equations (K_0 , K_1 and K_2 [day⁻¹] depending on whether SUZ is above a threshold value, UZL [mm], or not (Eq. 3). After adding percolation rate from the upper to the lower groundwater box (SLZ [mm]) with $PERC$ [mm day⁻¹] as maximum, the final streamflow is transformed by the parameter $MAXBAS$ [day] (Eq. 4) to give the modeled streamflow [mm day⁻¹].

$$Q_{Gw}(t) = K_2 \cdot SLZ + K_1 \cdot SUZ + K_0 \cdot \max(SUZ - UZL, 0), \tag{3}$$

$$Q_{sm}(t) = \sum_{i=1}^{MAXBAS} C(i)Q_{Gw}(t - i + 1), \tag{4}$$

where $C(i) = \int_{i-1}^i \left(\frac{2}{MAXBAS} - \left| u - \frac{MAXBAS}{2} \right| \times \frac{4}{MAXBAS^2} \right) du$, SUZ and SLZ are the water level filling the upper and lower reservoirs, respectively.

Model calibration, validation and performance assessment

Since the main hydrological processes in hydrological models are simplified by the model parameters that cannot be determined directly from field measurements, their calibration is required. Calibration is a technique that allows one to choose the best parameter set of the model, by adjusting manually or automatically their numerical values to more reproduce the response at the outlet (Madsen et al. 2002; Wu et al. 2012). The calibrated model parameters should necessarily be validated. Validation is

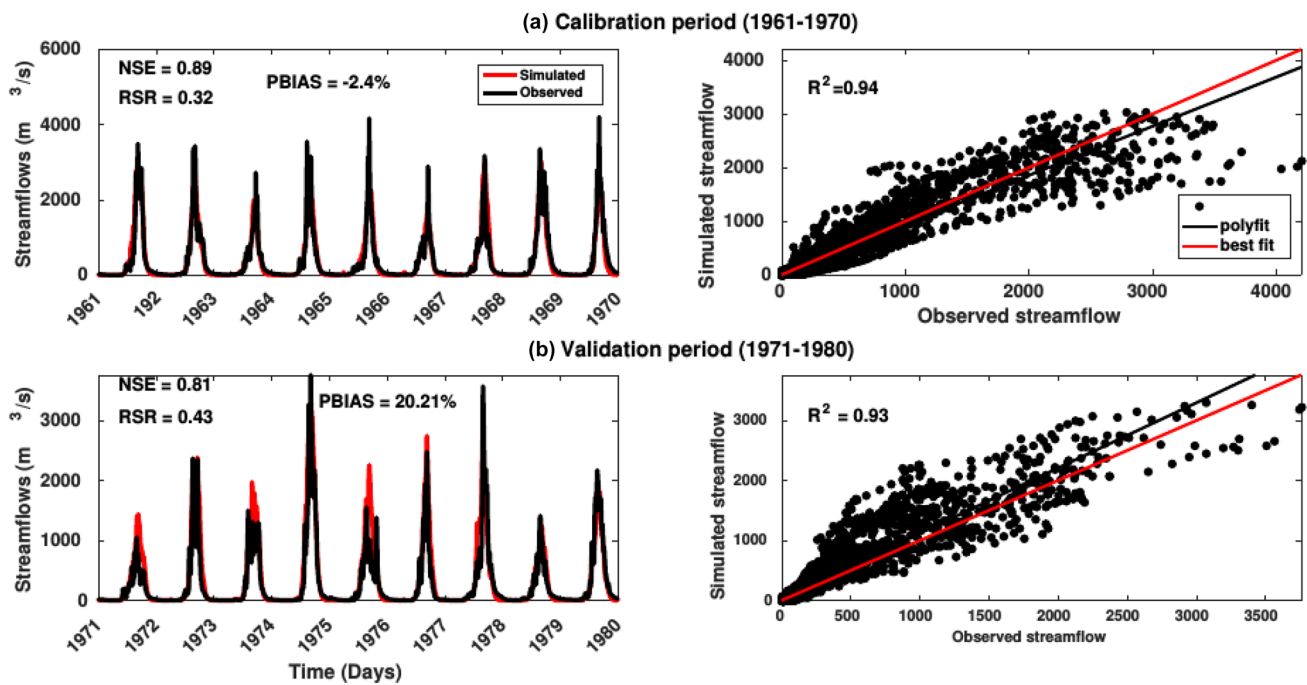


Fig. 2 Observed and simulated hydrographs (left panel) and scatter plot between the observed and modeled streamflows (right panel): calibration period (a) and validation period (b) in the gauging station Garoua

the process to check the reproducibility of the results by the calibrated parameters. A new dataset different from that in the phase of the calibration is used. In this study, we followed the split sample (SS) technique recommended by Klemeš (1986) and the Monte Carlo Simulations (Aghakouchak et al. 2013).

The model performance in the BRB was assessed by using performance criteria including Nash–Sutcliffe efficiency (NSE, Nash and Sutcliffe 1970), the coefficient of determination (R^2), the ratio between the root mean square error and observations standard deviation (RSR) and the percent bias (PBIAS). More details, equations and descriptions of those statistical techniques can be found in ASCE (1993; Legates and McCabe Jr 1999; Krause et al. 2005; Moriasi et al. 2007; Tegegne et al. 2017).

Method to estimate potential evapotranspiration

PET represents the evaporation capacity of the mass of the air when water is not a limiting factor. It is usually estimated by using air temperature, relative humidity, radiation and wind speed. But, in the data-scarce regions, these data are often not available in sufficient quantity over time. Several different mathematical formulas varying from temperature-based to physically based process methods have been developed, tested and applied to estimate PET for various types of land cover, water and vegetation (Thornthwaite 1948;

Penman 1956; Federer et al. 1996; Allen et al. 1998; Irmak et al. 2003).

In this study, the Hamon method (Hamon 1961) was used to estimate PET. Several studies found the Hamon method to well reproduce PET in different climate conditions (Federer et al. 1996; Vörösmarty et al. 1998; Lu et al. 2005; Legates and McCabe Jr 2005). This method was also used in recent CC impact studies (Yira et al. 2017; Tall et al. 2017). In the Hamon method, PET (mm day^{-1}) is estimated as:

$$\text{PET} = 715.5 \frac{N}{24} \frac{e_s(T_a)}{(T_a + 273.2)}, \quad (5)$$

where $e_s(T_a)$ is the saturated vapor pressure (KP_a) and N the daylight hours. Their equations can be found in Allen et al. (1998).

Results and discussion

Hydrological model evaluation

This section focuses on the ability of the HBV-Light hydrological model to simulate the streamflow in the BRB. Observed versus simulated hydrographs and statistical criteria obtained during the calibration and validation periods are presented in Fig. 2, while the best set of model parameters

obtained during the calibration can be found in Table 2. The model captures some important characteristics of streamflows in the BRB well such as the timing and intensity of high and low flows, although some bias still exists (Fig. 2). Figure 2 also shows that NSE and R^2 values are greater than 0.80 and 0.90, respectively, while *RSR* and *PBIAS* values are less than 0.50 and 20% respectively, during the calibration and validation of the model. According to Moriasi et al. (2007), the results reveal that the HBV-Light hydrological model simulates the daily streamflows in the BRB well. Thus, the optimized model parameters are representative for basin-scale hydrology of the BRB and can be used in the context of CC.

Remo model evaluation

This section describes the performance of the two outputs termed REMO–EC and REMO–MPI generated by the REMO model in simulating the present climate within the reference period 1983–2005. The annual cycle of precipitation, 2-m temperature, and estimated PET is shown in Fig. 3, while Table 3 summarizes the values of the different statistical criteria used. The reanalysis and observation data have similar variability of the annual cycle of monthly rainfall, 2-m temperature and PET over BRB, even though there exist some errors in time and magnitude. Most notable errors are found in the ERAINT and NCEP1 during the rainy season in which there are an over-estimation and under-estimation of rainfall respectively. When the magnitude of uncertainties in the observation and reanalysis data are taken into account, the REMO model represents the seasonality of temperature, PET and rainfall well with a unimodal character of rain (maximum obtained in August). Although the peak of rainfall intensity in all the two REMO simulations is lower compared with CRU and NCEP2 observation and reanalysis datasets, the REMO results sit within the spread of the combined reanalysis and CRU data. The annual cycle of 2-m temperature and PET do not exhibit a large variability between the different datasets (simulations and observations) as in case of mean monthly precipitation. In summer, the two REMO simulations overestimate the PET, while there is a stronger under-estimation of both 2-m temperature and PET during the September–October–November (SON) and December–January–February (DJF) seasons when compared to ERA and NCEP1. These results are reinforced by recent studies (Fotso-Nguemo et al. 2017b; Vondou and Haensler 2017; Tamoffo et al. 2019b), which demonstrated the ability of the REMO model to simulate well various aspects of the present climate such as daily, seasonal and annual cycle of precipitation over CA. In addition, Vondou and Haensler (2017) found that REMO model captures the variability in precipitation anomalies between different events associated with El Niño/Southern Oscillation, while Tamoffo

et al. (2019b) show that REMO adequately simulates the frequency of wet days, the threshold of extreme rainfall and the cumulative frequency of daily rainfall over CA.

Effect of climate change on the hydrological parameters of the BRB

This section focuses on the potential changes of precipitation, temperature, PET and streamflow by the near (2041–2065) and late (2071–2095) of the twenty-first century under RCPs 2.6, 4.5 and 8.5 relative to the baseline period (1981–2005).

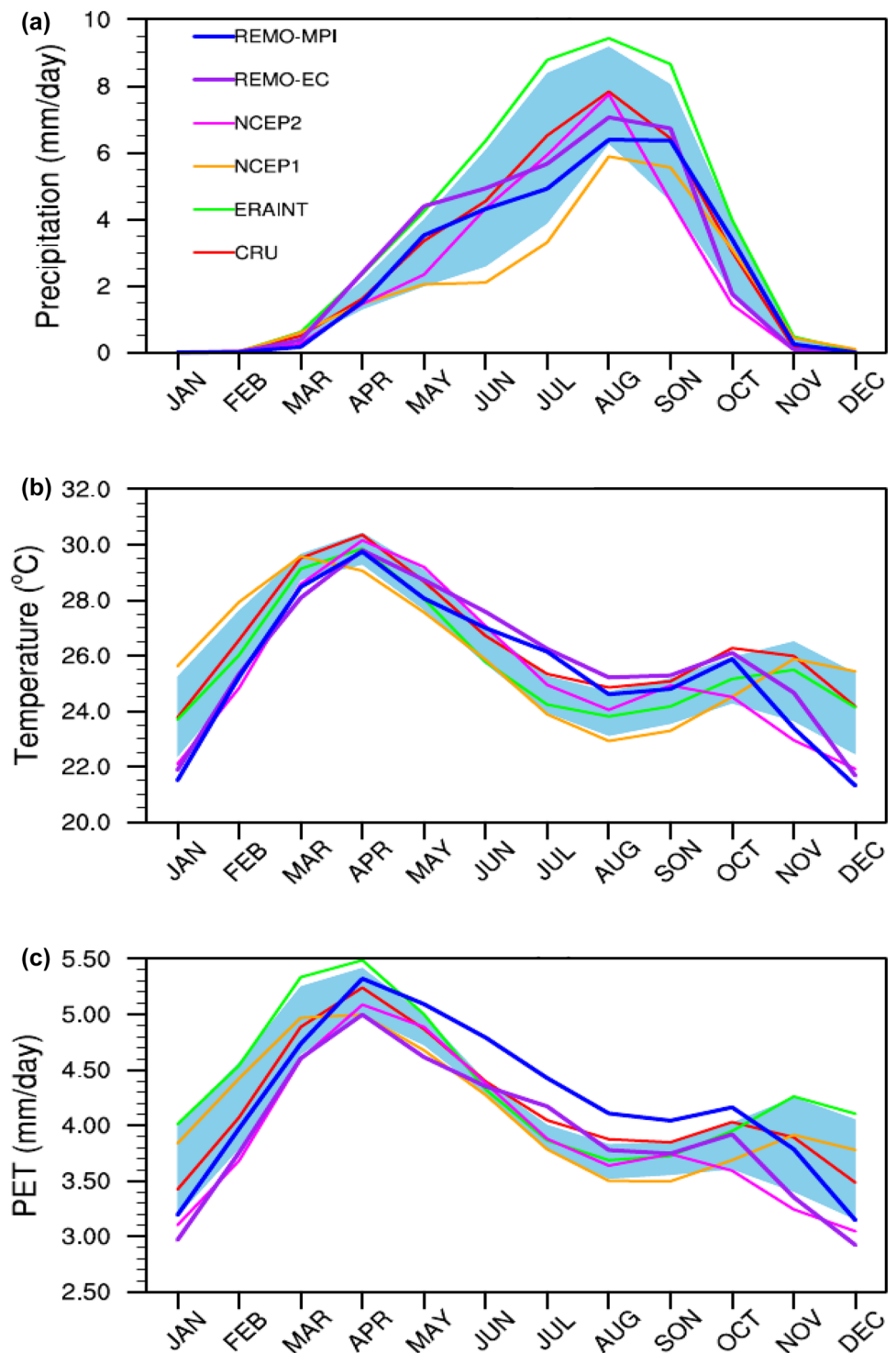
Changes in precipitation

The rainy season over the BRB extends from May to October with a maximum in August (see Fig. 3). Under RCP2.6 and RCP4.5, rainfall changes for the months May–August is uncertain as results are both weakly positive and negative depending on the driving GCM and future period (Fig. 4). However, under the RCP8.5 scenario, decreases in rainfall are projected in both the near and late future for these months. During September, large decreases in rainfall are projected under all scenarios in both time periods. The signal is strongest in the REMO–EC combination under RCP2.6, although in RCP8.5 both models show a strong decrease. During October, large increases in rainfall are projected by the REMO–EC model combination especially in the far future under RCPs 4.5 and 8.5. However, the REMO–MPI model combination projects effectively no change to a small decrease in rainfall in October rainfall. The projected change in October rainfall is, therefore, more uncertain than in September.

Seasonally, the signal changes with changing RCP. In RCP2.6 there is a projected decrease in MAM rainfall, an increase in JJA rainfall and a decrease in SON. In RCP4.5, there is a near-term increase but far-term decrease in MAM rainfall, smaller magnitudes in JJA changes than in RCP2.6 and a mixed signal of change in SON in both time slices. In RCP8.5, both near and far future show general decreases in rainfall in all seasons by most models. However, the SON season needs to be interpreted in the context of the monthly changes in September and October, particularly for the REMO–EC model combination that shows large, opposite signals in each respective month.

In summary, with increasing RCP, rainfall is projected to decrease during the rainy season with the largest impact during the key rainfall months of August and September under RCP8.5. The large projected increase in rainfall during October is only evident in one driving GCM (EC) so it should be interpreted with caution. A similar negative trend was reported by Mbaye et al. (2015) in the Upper Senegal Basin and Oguntunde and Abiodun (2013) in the NRB by using

Fig. 3 Climatological annual cycle of mean monthly precipitation (a), 2-m temperature (b) and PET (c) in all observation and reanalysis datasets (ERAINT, CRU, NCEP1 and NCEP2) and the REMO model simulations (REMO-EC and REMO-MPI) over BRB



REMO and RegCM4 RCMs, respectively. These results are also consistent with future dry conditions previously projected over CA (Fotso-Nguemo et al. 2017a, b; Sonkoué et al. 2018; Mba et al. 2018; Tamoffo et al. 2019a, b).

Changes in temperature and PET

Projected monthly, seasonal and annual temperature changes over BRB for the near and late twenty-first century under RCP2.6, RCP4.5 and RCP8.5 scenarios simulated with REMO-EC and REMO-MPI are presented in Fig. 5. In general, the temperature is projected to increase

Table 3 Summary of statistical evaluation of monthly precipitation (a), 2-m temperature (b) and PET (c) with the ERAINT, CRU, NCEP1 and NCEP2 data for the current 23-year period (1983–2005) over the BRB

	ERAINT			CRU			NCEP1			NCEP2		
	MB	R ²	RMSE	MB	R ²	RMSE	MB	R ²	RMSE	MB	R ²	RMSE
Precipitation												
REMO–EC	0.96	0.97	1.48	0.05	0.97	0.64	−0.52	0.90	1.43	−0.43	0.95	0.95
REMO–MPI	1.17	0.98	1.72	0.26	0.98	0.65	−0.73	0.96	0.95	−0.22	0.93	0.98
2-m temperature												
REMO–EC	1.95	0.54	3.03	0.88	0.88	2.18	0.86	0.57	2.34	−0.15	0.96	0.77
REMO–MPI	0.62	0.52	2.42	0.51	0.87	1.32	−0.47	0.54	2.26	−1.47	0.95	1.67
Potential evapotranspiration												
REMO–EC	0.43	0.69	0.64	0.24	0.95	0.31	0.18	0.71	0.48	−0.03	0.97	0.17
REMO–MPI	0.13	0.66	0.53	−0.06	0.94	0.24	−0.06	0.69	0.24	−0.12	0.97	0.50

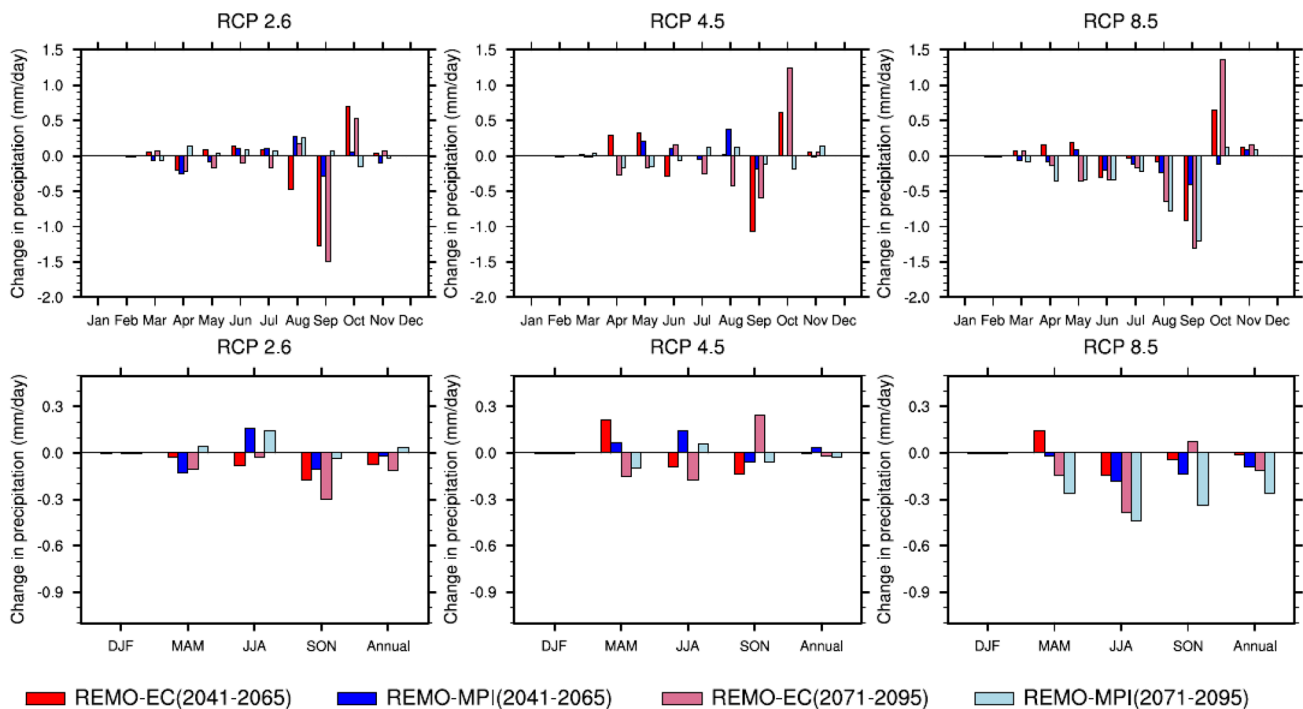


Fig. 4 Projected monthly (top), seasonal and annual (bottom) changes in precipitation over the BRB under the three scenarios (RCP2.6, RCP4.5, RCP8.5) for the two future periods (2041–2065 and 2071–2095) relative to the baseline period (1981–2005)

in all months and seasons under scenarios, models and future periods. In particular, under RCP2.6, the increase is lower than under RCP4.5 and RCP8.5, while RCP8.5 gave the highest value (up to 5 °C), as expected in higher equivalent CO₂ concentrations. The highest temperature increases were projected in the late twenty-first century under RCP4.5 and RCP8.5, whereas under RCP2.6 the highest temperature increases were projected in the near future with REMO–EC data. This feature is common to all multi-model ensembles studies performed in this

region (Kamga 2001; Oguntunde and Abiodun 2013; Fotso-Nguemo et al. 2017b; Mba et al. 2018).

The influence of CC on PET is similar to the pattern of changes in temperature with potential increase among scenarios, models and future periods (see Fig. S2). This result was expected given that temperature and PET are strongly correlated (Kamga 2001).

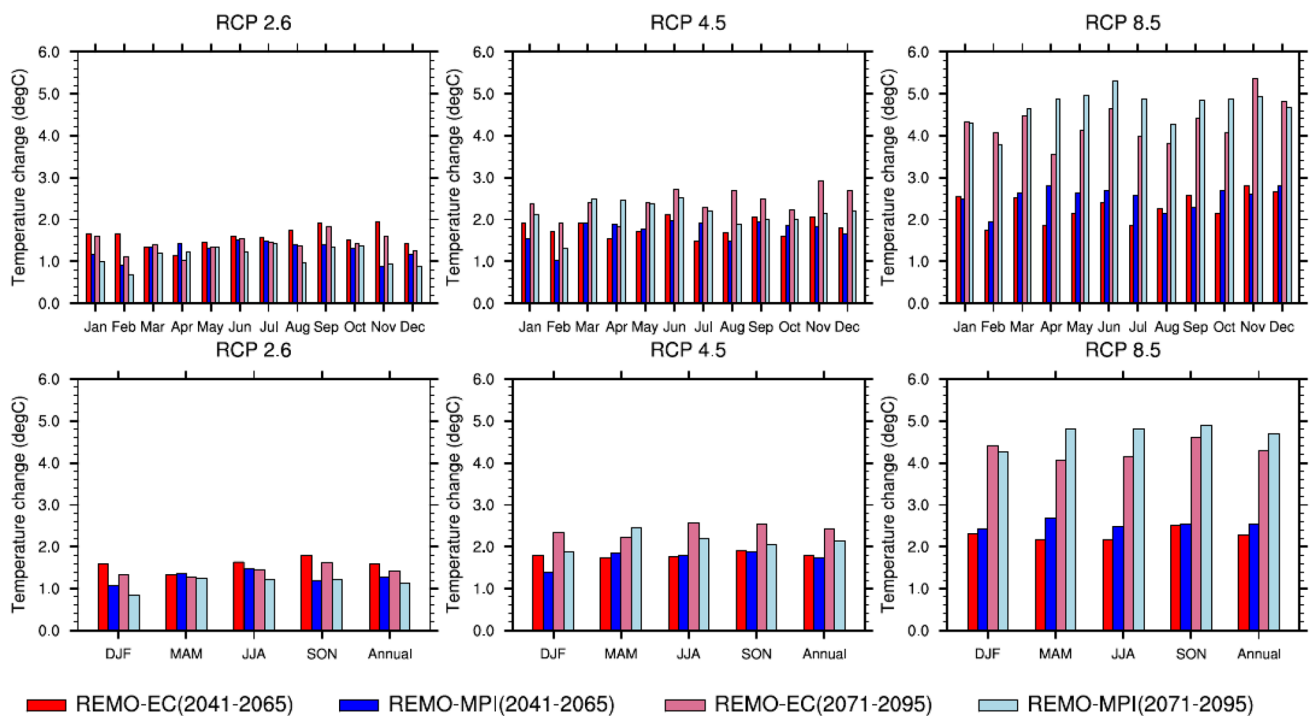


Fig. 5 Projected monthly (top), seasonal and annual (bottom) changes in temperature over the BRB under the three scenarios (RCP2.6, RCP4.5, RCP8.5) for the two future periods (2041–2065 and 2071–2095) relative to the baseline period (1981–2005)

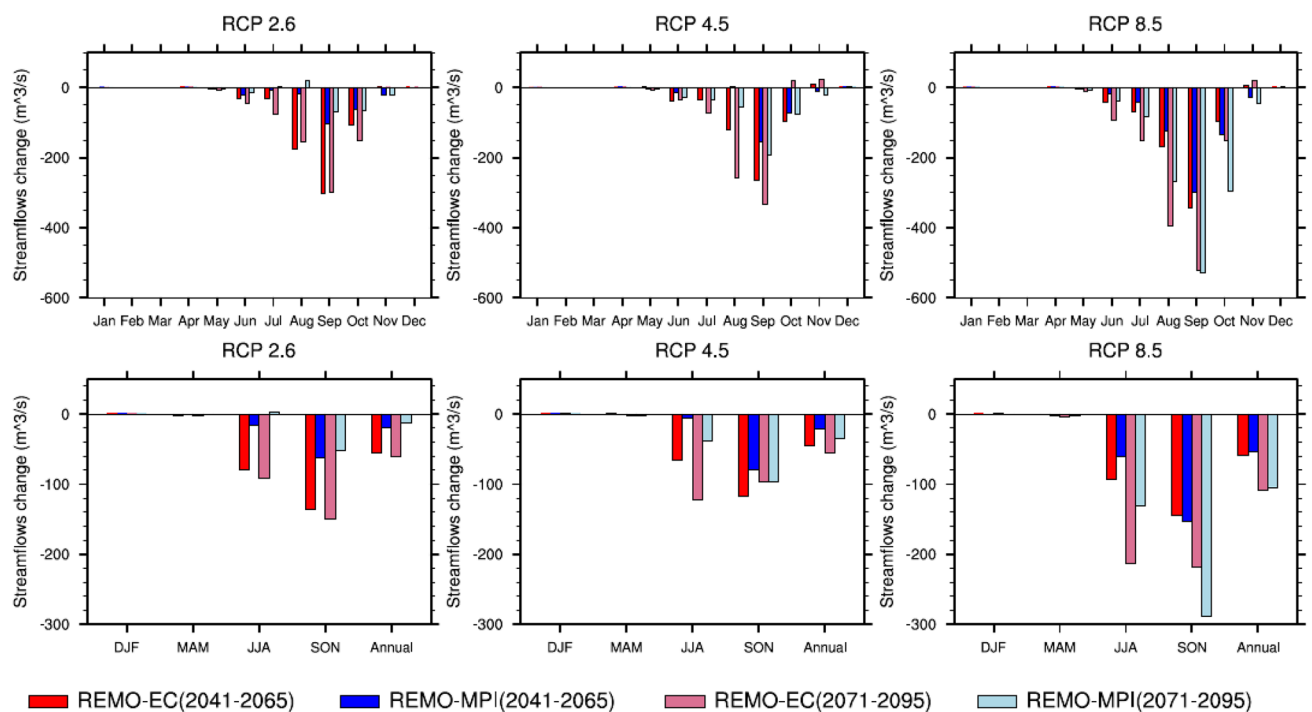


Fig. 6 Projected monthly (top), seasonal and annual (bottom) changes in Streamflow over the BRB under the three scenarios (RCP2.6, RCP4.5, RCP8.5) for the two future periods (2041–2065 and 2071–2095) relative to the baseline period (1981–2005)

Changes in streamflow

Figure 6 shows relative changes in monthly, seasonal and annual streamflow under the scenarios, models and time periods. Although there were some differences between scenarios, models and future periods, in general, streamflows are projected to decrease. During September, large decreases in streamflows are projected under all scenarios, models and future periods. The signal is strong in the REMO–MPI combination under RCP8.5 during the late of the twenty-first century. The dry months (November–April) do not exhibit a change signal which can be explained by the absence of rainfall during the period.

Seasonally, the sensitivity of streamflows to CC differed between the wet and dry seasons. In particular, a considerable decrease in streamflows is found in SON. Under those scenarios, seasons and time periods, the streamflow change is larger in the REMO–EC combination than that of the REMO–MPI combination, except under RCP8.5, which REMO–MPI predicted a larger streamflows change in SON. This can be explained since REMO–MPI projects a large change in rainfall than does REMO–EC in the same season (SON). The ranges of relative changes in annual streamflow are smaller than those in seasonal streamflow.

Although the decrease in annual streamflows increases with increased GHGs concentration scenario, the streamflow change under RCP2.6 is larger than that of RCP4.5 with REMO–EC in the two time periods. This result was expected because streamflow is usually very sensitive to changes in precipitation (as shown in Fig. 7) and the rainfall change under RCP2.6 is larger than the change under RCP4.5 with the same model. The results also reveal that the relative change in annual streamflows in the two time periods are relatively larger with REMO–EC under RCP2.6 and RCP4.5 than that of REMO–MPI, while under RCP8.5, the maximum annual decrease in streamflows is obtained with REMO–MPI simulations (Table 4). The projected late twenty-first century change in annual streamflows is larger than that in the mid twenty-first century under all scenarios and models except REMO–MPI under RCP2.6. This can be explained by the increase of precipitation in the near future with REMO–MPI under the same scenario and the change in streamflow is strongly correlated with the change in PET (Fig. 7) with the same model under the same scenario.

In summary, with increasing RCP, streamflow is projected to decrease during the rainy season with the largest impact during the key high flow month of September. The similar negative trend of streamflow was also found in several studies using the REMO model in Upper Senegal, Térou and

Ouéme catchments, respectively, by Mbaye et al. (2015), Cornelissen et al. (2013) and Bossa et al. (2014).

Compared to previous studies of the BRB (Kamga 2001; Sighomnou 2004), we produced opposite results. This can be explained given that streamflow can strongly relate to the combined change in precipitation and PET (Fig. 7). Kamga (2001) and Sighomnou (2004) found the increase of precipitation in the BRB by using HadCM2 and ECHAM4/OPYC3, respectively, which naturally project the increase of streamflows.

These findings demonstrate the importance of forcing hydrological models with higher resolution climate data for impact studies, and the need for regional climate information over Africa (Lennard et al. 2018) because Fotso-Nguemo et al. (2017a) found that GCMs (EC-Earth and MPI-ESM-LR) predict an increase of rainfall over CA, while the REMO model forced by those GCMs predict a decrease. A similar result was also reported by Oguntunde and Abiodun (2013) when comparing the RegCM3 RCM with ECHAM5 GCM.

Ecohydrologic analysis of the watershed

The ecohydrologic status of the watershed, known as a concept of water-energy budget (Tomer and Schilling 2009; Milne et al. 2002), is used to test the validity in assessing the interaction between increase PET and precipitation change as projected by the RCM-GCM model. It is determined by plotting the unused water (P_{ex}) against unused energy (E_{ex}) in the watershed (Yira et al. 2017). The shift in this status relative to the reference period detects the climate change signal, while the direction of the shift indicates whether the catchment experienced water stress or increased humidity. Figure 8 shows the ecohydrologic status of the BRB for time periods, models and scenarios. Figure 8 implies the drier environmental conditions of the watershed due to a decrease in excess water (precipitation) and an increase in evaporative demand. This led to a decrease of streamflow in the watershed and denotes an increase in PET higher than the increase in AET as reported in Table 4.

Drier environmental conditions of the watershed will be more evident under the RCP8.5 scenario than under the RCP4.5 and RCP2.6 scenarios, respectively. This can explain the important decrease of streamflow under the RCP8.5 scenario as shown in Fig. 6 and Table 4. The result also reveals that the REMO–MPI projects an extreme drier environmental condition than REMO–EC under RCP8.5. The same result was reported by Fotso-Nguemo et al. (2017b) over the CA region. This result can be reinforced by those found by Guenang and Kamga (2014) and Oguntunde et al. (2018). Guenang and Kamga (2014) have assessed the

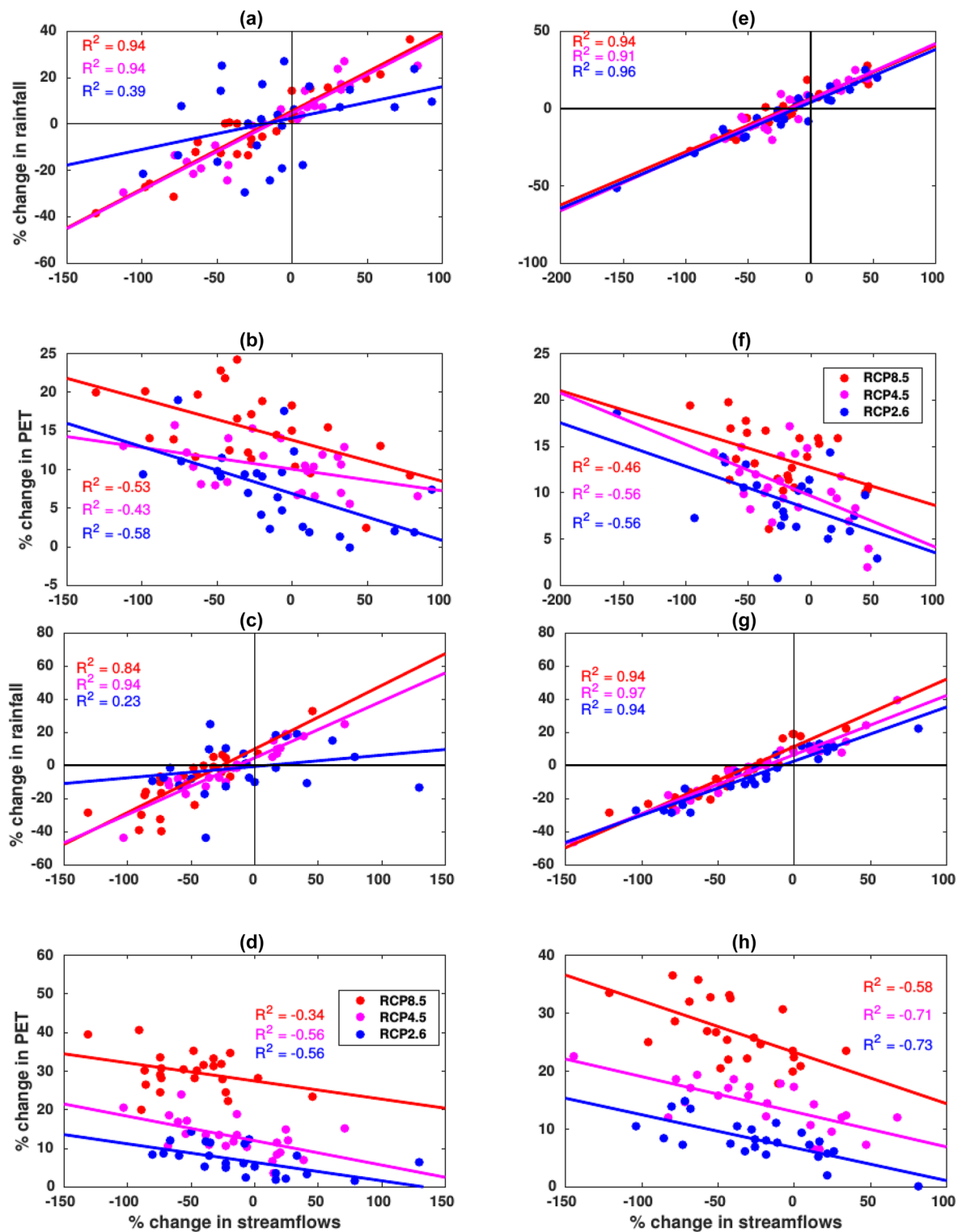


Fig. 7 Change in the inter-annual streamflow as a response to precipitation and PET change under emission scenarios RCP2.6, RCP4.5 and RCP8.5. Projected precipitation, PET and streamflow changes are calculated comparing period 1981–2005 to periods 2041–2065

(first and second lines of the panel) and 2071–2095 (third and fourth lines of the panel). REMO–MPI [first column of the panel (a–d)] and REMO–EC [second column of the panel (e–h)]

Table 4 Mean annual water balance components and percent change per RCM-GCM for the historical (1981–2005) and projected (2041–2065 and 2071–2095) periods under the RCP2.6, RCP4.5 and RCP8.5 scenarios

Water balance components	REMO-EC			REMO-MPI														
	Baseline			RCP2.6		RCP4.5		RCP8.5		Baseline		RCP2.6		RCP4.5		RCP8.5		
	Value	%	%	Value	%	Value	%	Value	%	Value	%	Value	%	Value	%	Value	%	
Mid twenty-first century (2041–2065)																		
Precipitation (mm/year)	1020.5	995.26	-2.48	1020.6	00	1016.9	-0.35	952.7	945.87	-0.71	966.55	1.45	920.98	-3.33				
PET (mm/year)	1456.9	1586.6	8.90	1610.2	10.53	1653.5	13.49	1567	1682.2	7.37	1725.5	10.11	1802.6	15.04				
AET (mm/year)	738.71	765.70	3.65	786.56	6.48	790.51	7.01	733.88	751.43	2.39	768.55	4.72	760.51	3.62				
Soil moisture (mm/year)	158.99	150.35	-5.43	152.53	-4.06	149.11	-6.21	147.88	140.82	-4.77	139.9	-5.39	133.25	-9.89				
Streamflow (mm/year)	273.16	218.53	-20.0	227.87	-16.58	213.44	-21.86	207.39	187.58	-9.55	186.03	-10.3	153.07	-26.19				
Late twenty-first century (2071–2095)																		
Precipitation (mm/year)	1020.5	981.41	-3.83	1013.4	-0.69	979.25	-4.04	952.7	965.45	1.33	944.05	-0.9	858.18	-9.92				
PET (mm/year)	1456.9	1575.5	8.14	1664.2	14.23	1845.8	26.69	1567	1669.3	6.52	1766.9	12.76	2029.2	29.49				
AET (mm/year)	738.71	754.62	2.15	788.76	6.78	805.58	9.05	733.88	760.08	3.57	757.60	3.23	752.70	2.56				
Soil moisture (mm/year)	158.99	149.84	-5.75	148.30	-6.72	136.91	-13.88	147.88	142.87	-3.38	135.79	-8.17	116.27	-21.03				
Streamflow (m ³ /s)	273.16	211.94	-22.4	217.71	-20.3	164.33	-39.84	207.39	194.49	-6.22	173.17	-16.5	101.49	-51.06				

drought occurrences in Cameroon over recent decades and found that the drought magnitude and duration increased with time for both short and long timescales in the North of Cameroon, as a response of a reduction in precipitation due to CC. Oguntunde et al. (2018) have studied the impacts of climate variability and change on drought characteristics in the NRB and found an increase in drought intensity and frequency over the NRB as a result of statistically significant correlation between runoff and drought indices.

Summary and conclusions

In the area where rainfed agriculture is the most important socioeconomic activity and where hydropower is the major source of electricity production, impact studies of future water resources are highly important for adaptation, or for inclusion in the design of new systems purpose. The main focus of this work was to evaluate the influence of the projected temperature and precipitation change on water resources in the BRB, Northern Cameroon. Streamflow was produced by coupling dynamically downscaled precipitation and temperature from the REMO model and the HBV-Light hydrological model under three (GHGs) concentration scenarios (RCP2.6, RCP4.5, and RCP8.5) during the future and baseline periods. The main findings of this research are:

1. The best set of optimized model parameters of the HBV-Light hydrological model obtained by using the Monte Carlo simulations during the model calibration was found to be representative for basin-scale hydrology of the BRB. Therefore, the HBV-Light hydrological model could effectively simulate the hydrological components change in the BRB.
2. The ability of the REMO model to simulate the present climate was evaluated prior to future climate change impact assessment. The REMO model was found to reproduce the annual cycle of rainfall, 2-m temperature and PET well, although some relative low biases still exist (MB less than 1 mm/day). The correlation coefficient between the REMO model and reanalysis (ERAINT, NCEP1, NCEP2) and observation (CRU) datasets are around 0.95 for precipitation.
3. Annual temperature and PET are projected to consistently increase under all scenarios, models and future periods. Although there is some uncertainty, annual precipitation is generally projected to decrease in the BRB up to 10% under the RCP8.5 scenario in the late twenty-first century. This potential increase of both temperature and PET and a decrease of precipitation may lead to a decrease in the soil moisture (Fig. S3) and the increase of water stress of the plants. The agricultural production is likely to decline and with the decline of

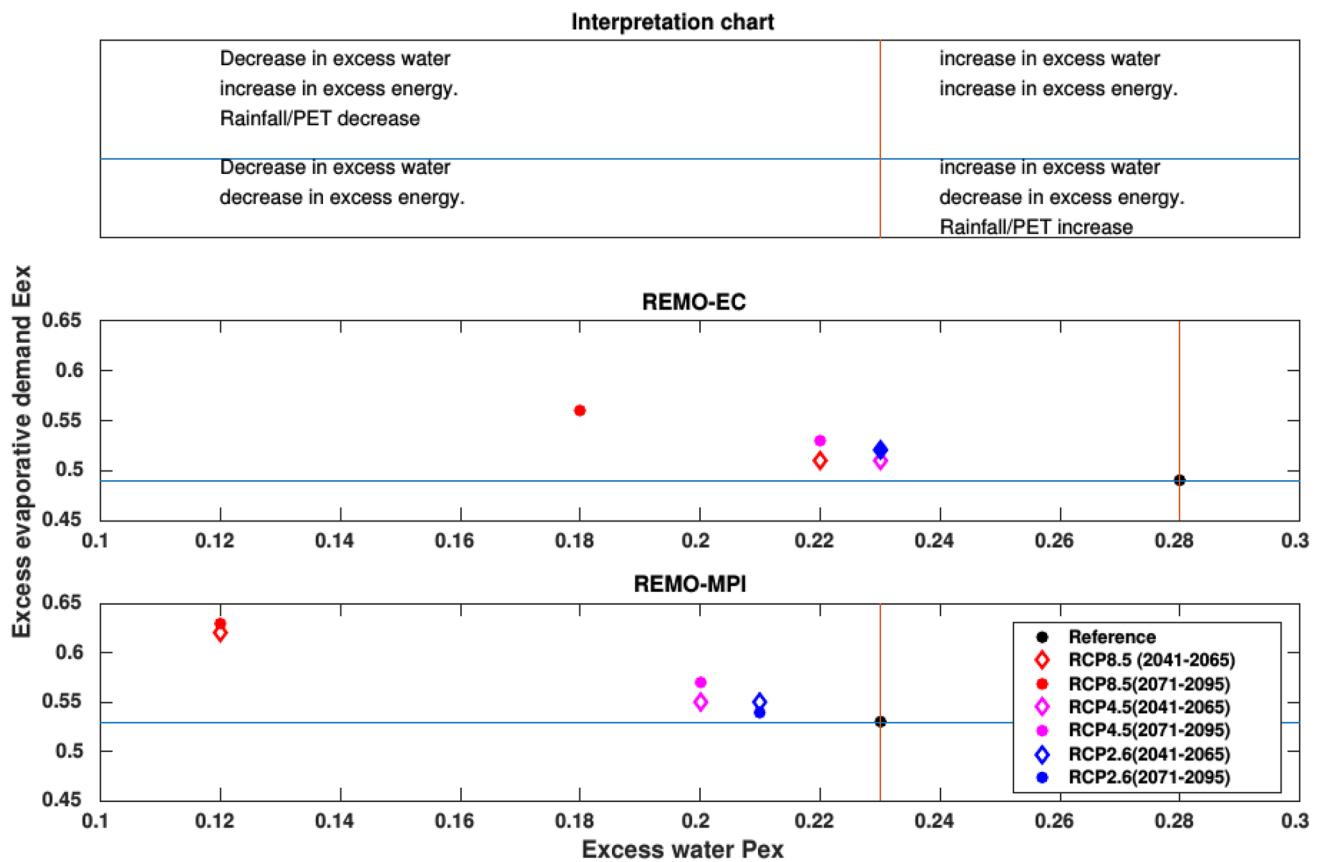


Fig. 8 Plot of excess precipitation (P_{ex}) vs. evaporative demand (E_{ex}) for the reference period (1981–2005) and emission scenarios RCP2.6, RCP4.5 and RCP8.5 [2041–2065 (diamond) and 2071–2095 (filled circle)] for the REMO–MPI and REMO–EC. The shift in RCP dots

compared to the reference period's dot indicates the effects of climate change on the catchment hydrology. P_{ex} and E_{ex} for each period are calculated from the annual average rainfall, PET and AET

vegetation cover, the amplification of desertification in this area will increase.

4. The combination of reduced precipitation increased PET and reduced soil moisture, resulting in a decrease in streamflow in the BRB. This important decrease of streamflow will also negatively affect the hydropower potential of the Lagdo Dam, water irrigation and navigation in both future periods and importantly will move the region into a drier environmental conditions as shown by $(E_{ex})-(P_{ex})$ plot.

One major caveat of this study is that only one RCM has been used. Likewise, results indicate that rainfall change in October is uncertain with contrasting runs' signal. Therefore, further works with a multi-model ensemble from CORDEX-Africa matrix are needed to quantify the range of uncertainty in this signal. Nevertheless, this study highlights the importance of using RCMs instead of GCMs for impact studies. Moreover, results might be useful for decision makers and planners in developing adaptation

strategies so as to limit the risks associated with global warming.

Acknowledgements The authors would like to thank Pr Amir Aghakouchak at the Department of Civil Engineering at The University of Louisiana at Lafayette (USA) for his technical support. The authors also thank projects and institutions which provided datasets. We also acknowledge logistical support from the CORDEX International Project Office, the Swedish Meteorological and Hydrological Institute and the Climate System Analysis Group at the University of Cape Town. The authors gratefully acknowledge the comments of the reviewers and the editor, which enormously improved the presentation of the final manuscript.

Compliance with ethical standards

Conflict of interest The authors declare that they have no competing interest.

References

- Abebe NA, Ogden FL, Pradhan NR (2010) Sensitivity and uncertainty analysis of the conceptual HBV rainfall–runoff model: implications for parameter estimation. *J Hydrol* 389(3):301–310. <https://doi.org/10.1016/j.jhydrol.2010.06.007>
- Aghakouchak A, Habib E (2010) Application of a conceptual hydrologic model in teaching hydrologic processes. *Int J Eng Educ* 26:963–973
- Aghakouchak A, Nakhjiri N, Habib E (2013) An educational model for ensemble streamflow simulation and uncertainty analysis. *Hydrol Earth Syst Sci* 17(2):445–452. <https://doi.org/10.5194/hess-17-445-2013>
- Aich V, Liersch S, Vetter T, Huang S, Tecklenburg J, Hoffmann P, Koch H, Fournet S, Krysanova V, Muller EN, Hattermann FF (2014) Comparing impacts of climate change on streamflow in four large African river basins. *Hydrol Earth Syst Sci* 18(4):1305–1321. <https://doi.org/10.5194/hess-18-1305-2014>
- Aich V, Liersch S, Vetter T, Fournet S, Andersson JC, Calmanti S, van Weert FH, Hattermann FF, Paton EN (2016) Flood projections within the Niger River Basin under future land use and climate change. *Sci Total Environ* 562:666–677. <https://doi.org/10.1016/j.scitotenv.2016.04.021>
- Alamou EA, Obada E, Afouda A (2017) Assessment of future water resources availability under climate change scenarios in the Mékrou Basin. *Hydrology, Benin*. <https://doi.org/10.3390/hydrology4040051>
- Allen RG, Pereira LS, Raes D, Smith M (1998) Crop evapotranspiration—guidelines for computing crop water requirements. *FAO Irrigation and drainage paper* 56, FAO, Rome, pp. 300
- Aloysius N, Saiers J (2017) Simulated hydrologic response to projected changes in precipitation and temperature in the Congo River Basin. *Hydrol Earth Syst Sci* 21:4115–4130. <https://doi.org/10.5194/hess-2016-152>
- ASCE (1993) Criteria for evaluation of watershed models. *J Irrig Drain Eng* 119:429–442
- Bajracharya AR, Bajracharya SR, Shrestha AB, Maharjan SB (2018) Climate change impact assessment on the hydrological regime of the Kaligandaki Basin, Nepal. *Sci Total Environ* 625:837–848. <https://doi.org/10.1016/j.scitotenv.2017.12.332>
- Bergstrom S (1976) Development and Application of a Conceptual Runoff Model for Scandinavian Catchments. Report RHO 7, Swedish Meteorological and Hydrological Institute, Norrköping, Sweden, p 134
- Bossa AY, Diekkrüger B, Agbossou EK (2014) Scenario-based impacts of land use and climate change on land and water degradation from the meso to regional scale. *Water* 6(10):3152–3181. <https://doi.org/10.3390/w6103152>
- Cheo AE, Voigt HJ, Mbua RL (2013) Vulnerability of water resources in Northern Cameroon in the context of climate change. *Environ Earth Sci* 70(3):1211–1217. <https://doi.org/10.1007/s12665-012-2207-9>
- Chisholm H (1911) *Benue*. *Encyclopaedia Britannica* 3, 11th edn. Cambridge University Press, Cambridge, p 754
- Chou SC, Lyra A, Mourão C, Dereczynski C, Pilotto I, Gomes J, Bustamante J, Tavares P, Silva A, Rodrigues D, Campos D, Chagas D, Sueiro G, Siqueira G, Marengo J (2014) Assessment of climate change over South America under RCP4.5 and 8.5 downscaling scenarios. *Am J Clim Change* 3(5):512–525
- Cornelissen T, Diekkrüger B, Gieritz S (2013) A comparison of hydrological models for assessing the impact of land use and climate change on discharge in a tropical catchment. *J Hydrol* 498:221–236. <https://doi.org/10.1016/j.jhydrol.2013.06.016>
- Coulibaly N, Coulibaly TJH, Mpakama Z, Savané I (2018) The impact of climate change on water resource availability in a trans-boundary basin in West Africa: the case of Sassandra. *Hydrology*. <https://doi.org/10.3390/hydrology5010012>
- Deb D, Butcher J, Srinivasan R (2015) Projected hydrologic changes under mid-21st century climatic conditions in a sub-arctic watershed. *Water Resour Manag* 29(5):1467–1487. <https://doi.org/10.1007/s11269-014-0887-5>
- Dee D, Uppala SM, Simmons AJ, Berrisford P, Poli P, Kobayashi S, Andrae U, Balmaseda M, Balsamo G, Bauer P, Bechtold P, Beljaars A, van de Berg L, Bidlot J, Bormann N, Delsol C, Dragani R, Fuentes M, Geer AJ, Haimberger L, Healy S, Hersbach H, Ho'lm EV, Isaksen L, Kallberg P, Köhler M, Matricardi M, McNally AP, Monge-Sanz BM, Morcrette JJ, Park BK, Peubey C, de Rosnay P, Tavolato C, Thépaut JN, Fal Vitart (2011) The ERA-Interim reanalysis: configuration and performance of the data assimilation system. *Q J R Meteorol Soc* 137:553–597. <https://doi.org/10.1002/qj.828>
- El-Khoury A, Seidou O, Lapen D, Que Z, Mohammadian M, Sunohara M, Bahram D (2015) Combined impacts of future climate and land use changes on discharge, nitrogen and phosphorus loads for a Canadian river basin. *J Environ Manag* 151:76–86. <https://doi.org/10.1016/j.jenvman.2014.12.012>
- Federer CA, Vorosmarty C, Fekete B (1996) Intercomparison of methods for calculating potential evaporation in regional and global water balance models. *Water Resour Res* 32(7):2315–2321
- Fotso-Nguemo TC, Vondou DA, Pokam MW, Yepdo DZ, Ismaïlla D, Haensler A, Tchotchou DLA, Kamsu-Tamo PH, Gaye TA, Tchawoua C (2017a) On the added value of the regional climate model REMO in the assessment of climate change signal over Central Africa. *Clim Dyn* 49(11):3813–3838. <https://doi.org/10.1007/s00382-017-3547-7>
- Fotso-Nguemo TC, Vondou DA, Tchawoua C, Haensler A (2017b) Assessment of simulated rainfall and temperature from the regional climate model REMO and future changes over Central Africa. *Clim Dyn* 48(11):3685–3705. <https://doi.org/10.1007/s00382-016-3294-1>
- Gao H, Bohn TJ, Podest E, McDonald KC, Lettenmaier DP (2011) On the causes of the shrinking of Lake Chad. *Environ Res Lett* 6(3):034021. <http://stacks.iop.org/1748-9326/6/i=3/a=034021>. Accessed July–Aug 2019
- Giorgi F, Jones C, Asrar GR et al (2009) Addressing climate information needs at the regional level: the cordex framework. *World Meteorol Org (WMO) Bull* 58(3):175
- Guenang GM, Kamga FM (2012) Onset, retreat and length of the rainy season over Cameroon. *Atmos Sci Lett* 13:120–127. <https://doi.org/10.1002/asl.371>
- Guenang GM, Kamga FM (2014) Computation of the standardized precipitation index (SPI) and its use to assess drought occurrences in Cameroon over recent decades. *J Appl Meteorol Climatol* 53(10):2310–2324. <https://doi.org/10.1175/JAMC-D-14-0032.1>
- Hagemann S (2002) An Improved Land Surface Parameter Dataset for Global and Regional Climate Models. MPI Report No 336; Max-Planck-Institute for Meteorology: Hamburg, Germany
- Hamon WR (1961) Estimating potential evapotranspiration. *J Hydraul Div Proc Am Soc Civil Eng* 87:107–120
- Harris I, Jones P, Osborn T, Lister D (2014) Updated high-resolution grids of monthly climatic observations—the CRUTS3.10 dataset. *Int J Climatol* 34:623–642. <https://doi.org/10.1002/joc.3711>
- IPCC (2013) *Climate Change 2013 The Physical Scientific Basis*, IPCC Contribution of Working Group I to the Fifth Assessment Report of the Intergovernmental Panel on Climate Change. Cambridge University Press, Cambridge

- Irmak S, Irmak A, Allen RG, Jones JW (2003) Solar and Net Radiation-Based Equations to Estimate Reference Evapotranspiration in Humid Climates. *J Irrig Drain Eng* 123:336–347
- Jacob D (2001) A note to the simulation of the annual and inter-annual variability of the water budget over the Baltic Sea drainage basin. *Meteorol Atmos Phys* 77(1):61–73. <https://doi.org/10.1007/s007030170017>
- Jacob D, Elizalde A, Haensler A, Hagemann S, Kumar P, Podzun R, Rechid D, Remedio AR, Saeed F, Sieck K, Teichmann C, Wilhelm C (2012) Assessing the transferability of the regional climate model REMO to different coordinated regional climate downscaling experiment (CORDEX) regions. *Atmosphere* 3(1):181–199. <https://doi.org/10.3390/atmos3010181>
- Kalnay E, Kanamitsu M, Kistler R, Collins W, Deaven D, Gandin L, Iredell M, Saha S, White G, Woollen J, Zhu Y, Chelliah M, Ebisuzaki W, Higgins W, Janowiak J, Mo KC, Ropelewski C, Wang J, Leetmaa A, Reynolds R, Jenne R, Joseph D (1996) The NCEP/NCAR 40-year reanalysis project. *Bull Am Meteorol Soc* 77(3):437–472. [https://doi.org/10.1175/1520-0477\(1996\)0770437:TNYRP2.0.CO;2](https://doi.org/10.1175/1520-0477(1996)0770437:TNYRP2.0.CO;2)
- Kamga FM (2001) Impact of greenhouse gas induced climate change on the runoff of the Upper Benue River (Cameroon). *J Hydrol* 252(1):145–156. [https://doi.org/10.1016/S0022-1694\(01\)00445-0](https://doi.org/10.1016/S0022-1694(01)00445-0)
- Kanamitsu M, Ebisuzaki W, Woollen J, Yang SK, Hnilo JJ, Fiorino M, Potter GL (2002) NCEP–DOE AMIP-II reanalysis (R-2). *Bull Am Meteorol Soc* 83(11):1631–1644. <https://doi.org/10.1175/BAMS-83-11-1631>
- Khan MYA, Gani KM, Chakrapani GJ (2015) Assessment of surface water quality and its spatial variation. A case study of Ramganga River, Ganga Basin, India. *Arab J Geosci* 9(1):28. <https://doi.org/10.1007/s12517-015-2134-7>
- Khan MYA, Daityari S, Chakrapani GJ (2016a) Factors responsible for temporal and spatial variations in water and sediment discharge in Ramganga River, Ganga Basin, India. *Environ Earth Sci* 75(4):283. <https://doi.org/10.1007/s12665-015-5148-2>
- Khan MYA, Khan B, Chakrapani GJ (2016b) Assessment of spatial variations in water quality of Garra River at Shahjahanpur, Ganga Basin, India. *Arab J Geosci* 9(8):516. <https://doi.org/10.1007/s12517-016-2551-2>
- Klemeš V (1986) Operational testing of hydrologic simulation models. *Hydrol Sci J* 31(1):13–24
- Krause P, Boyle DP, Bäse F (2005) Comparison of different efficiency criteria for hydrological model assessment. *Adv Geosci* 5:89–97. <https://hal.archives-ouvertes.fr/hal-00296842>. Accessed July–Aug 2019
- Legates DR, McCabe GJ Jr (1999) Evaluating the use of goodness-of-fit measures in hydrologic and hydroclimatic model validation. *Water Resour Res* 135(1):233–241. <https://doi.org/10.1029/1998WR900018>
- Legates DR, McCabe CJ (2005) A re-evaluation of the average annual global water balance. *Phys Geogr* 26:467–479
- Lennard CJ, Nikulin G, Dosio A, Moufouma-Okia W (2018) On the need for regional climate information over Africa under varying levels of global warming. *Environ Res Lett* 13(6):060401. <https://doi.org/10.1088/1748-9326/aab2b4>
- Leta OT, El-Kadi AI, Dulai H, Ghazal KA (2016) Assessment of climate change impacts on water balance components of Heeia watershed in Hawaii. *J Hydrol Reg Stud* 8:182–197. <https://doi.org/10.1016/j.ejrh.2016.09.006>
- Li L, Diallo I, Xu CY, Stordal F (2015) Hydrological projections under climate change in the near future by RegCM4 in Southern Africa using a large-scale hydrological model. *J Hydrol* 528:1–16. <https://doi.org/10.1016/j.jhydrol.2015.05.028>
- Lohmann U, Roeckner E (1996) Design and performance of a new cloud microphysics scheme developed for the ECHAM general circulation model. *Clim Dyn* 12(8):557–572. <https://doi.org/10.1007/BF00207939>
- Louis JF (1979) A parametric model of vertical eddy fluxes in the atmosphere. *Bound-Layer Meteorol* 17(2):187–202. <https://doi.org/10.1007/BF00117978>
- Lu J, Sun G, McNulty SG, Amataya DM (2005) A comparison of six potential evapotranspiration methods for regional use in the Southeastern United States. *J Am Water Resour Assoc* 3:621–633
- Madsen H, Wilson G, Ammentorp HC (2002) Comparison of different automated strategies for calibration of rainfall-runoff models. *J Hydrol* 261(1):48–59. [https://doi.org/10.1016/S0022-1694\(01\)00619-9](https://doi.org/10.1016/S0022-1694(01)00619-9)
- Mba WP, Longandjo GNT, Moufouma-Okia W, Bell JP, James R, Vondou DA, Haensler A, Fotso-Nguemo TC, Guenang GM, Tchotchou ALD, Kamsu-Tamo PH, Takong RR, Nikulin G, Lennard CJ, Dosio A (2018) Consequences of 1.5°C and 2°C global warming levels for temperature and precipitation changes over Central Africa. *Environ Res Lett* 13(5):055011. <https://doi.org/10.1088/1748-9326/aab048>
- Mbaye ML, Hagemann S, Haensler A, Stacke T, Gaye AT, Afouda A (2015) Assessment of climate change impact on water resources in the Upper Senegal Basin (West Africa). *Am J Clim Change* 4:77–93. <https://doi.org/10.4236/ajcc.2015.41008>
- Meng F, Su F, Yang D, Tong K, Hao Z (2016) Impacts of recent climate change on the hydrology in the source region of the Yellow River Basin. *J Hydrol Reg Stud* 6:66–81. <https://doi.org/10.1016/j.ejrh.2016.03.003>
- Milne BT, Gupta VK, Restrepo C (2002) A scale invariant coupling of plants, water, energy, and terrain. *Ecoscience* 9(2):191–199. <https://www.jstor.org/stable/42901483>. Accessed 1 Aug 2019
- Mohammadzadeh N, Amiri JB, Endergoli EL, Karimi S (2019) Coupling Tank model and LARS-Weather generator in assessments of the impacts of climate change on water resources. *Slovak J Civil Eng* 27(1):14–24. <https://doi.org/10.2478/sjce-2019-0003>
- Molua EL, Lambi CM (2006) Climate, hydrology and water resources in Cameroon. Discussion Paper No 33 Special Series on Climate Change and Agriculture in Africa, University of Pretoria, Pretoria: Centre for Environmental Economics and Policy in Africa (CEEPA)
- Molua EL, Lambi CM (2007) The economic impact of climate change on agriculture in Cameroon. Policy Research Working Paper 4364, World Bank. <http://econ.worldbank.org>
- Morcrette JJ (1991) Radiation of cloud radiative properties in the European Centre for medium range weather forecasts forecasting system. *J Geophys Res* 96(5):9121–9132
- Moriasi DN, Arnold JG, Van Liew MW, Bingner RL, Harmel RD, Veith TL (2007) Model evaluation guidelines for systematic quantification of accuracy in watershed simulations. *Trans ASABE* 50:885–900
- Nash J, Sutcliffe J (1970) River flow forecasting through conceptual models part I—a discussion of principles. *J Hydrol* 10(3):282–290. [https://doi.org/10.1016/0022-1694\(70\)90255-6](https://doi.org/10.1016/0022-1694(70)90255-6)
- Nilawar AP, Waikar ML (2018) Use of SWAT to determine the effects of climate and land use changes on streamflow and sediment concentration in the Purna River Basin, India. *Environ Earth Sci* 77(23):783. <https://doi.org/10.1007/s12665-018-7975-4>
- Obeysekera J, Irizarry M, Park J, Barnes J, Dessalegne T (2011) Climate change and its implications for water resources management in South Florida. *Stoch Environ Res Risk Assess* 25(4):495–516. <https://doi.org/10.1007/s00477-010-0418-8>
- Oguntunde PG, Abiodun BJ (2013) The impact of climate change on the Niger River Basin hydroclimatology, West Africa. *Clim Dyn* 40(1):81–94. <https://doi.org/10.1007/s00382-012-1498-6>
- Oguntunde PG, Lischeid G, Abiodun BJ (2018) Impacts of climate variability and change on drought characteristics in the Niger

- River Basin, West Africa. *Stoch Environ Res Risk Assess* 32(4):1017–1034. <https://doi.org/10.1007/s00477-017-1484-y>
- Oyerinde GT, Hountondji FCC, Lawin AE, Odojin AJ, Afouda A, Diekkruiger B (2017) Improving hydro-climatic projections with bias-correction in Sahelian Niger Basin. *Climate, West Africa*. <https://doi.org/10.3390/cli5010008>
- Penlap KE, Matulla C, Storch HV, Mkankam Nkamga F (2004) Downscaling of GCM scenarios to assess precipitation changes in the little rainy season (March–June) in Cameroon. *Clim Res* 26:85–96
- Penman HL (1956) Evaporation: an introductory survey. *Neth J Agr Sci* 1:9–29
- Riahi K, Rao S, Krey V, Cho C, Chirkov V, Fischer G, Kindermann G, Nakicenovic N, Rafaj P (2011) RCP 8.5—a scenario of comparatively high greenhouse gas emissions. *Clim Change* 109(1):33. <https://doi.org/10.1007/s10584-011-0149-y>
- Boyer JF, Dieulin C, Rouche N, CRES A, Servat E, Paturel JE, Mahé G (2006) SIEMEM: an environmental information system for water resources. In: 5th World FRIEND Conference, La Havana–Cuba, November 2006 in Climate Variability and Change—Hydrological Impacts IAHS Publ 308:19–25
- Roudier P, Ducharme A, Feyen L (2014) Climate change impacts on runoff in West Africa: a review. *Hydrol Earth Syst Sci* 18:2789–2801. <https://doi.org/10.5194/hess-18-2789-2014>
- Sada R, Schmalz B, Kiesel J, Fohrer N (2019) Projected changes in climate and hydrological regimes of the Western Siberian lowlands. *Environ Earth Sci* 78(2):56. <https://doi.org/10.1007/s12665-019-8047-0>
- Sahoo GB, Schladow SG, Reuter JE, Coats R (2011) Effects of climate change on thermal properties of lakes and reservoirs, and possible implications. *Stoch Environ Res Risk Assess* 25(4):445–456. <https://doi.org/10.1007/s00477-010-0414-z>
- Saidi H, Dresti C, Manca D, Ciampittiello M (2018) Quantifying impacts of climate variability and human activities on the streamflow of an Alpine River. *Environ Earth Sci* 77(19):690. <https://doi.org/10.1007/s12665-018-7870-z>
- Sakho S, Dupont JP, Cisse MT, Loum S (2017) Hydrological responses to rainfall variability and dam construction: a case study of the Upper Senegal River basin. *Environ Earth Sci* 76:253. <https://doi.org/10.1007/s12665-017-6570-4>
- Seibert J (1999) Regionalisation of parameters for a conceptual rainfall-runoff model. *Agr Forest Meteorol* 98–99:279–293. [https://doi.org/10.1016/S0168-1923\(99\)00105-7](https://doi.org/10.1016/S0168-1923(99)00105-7)
- Seibert J (2005) HBV light version 2, User's manual. Stockholm University, Stockholm
- Seibert J, Vis MJP (2012) Teaching hydrological modeling with a user-friendly catchment-runoff-model software package. *Hydrol Earth Syst Sci* 16(9):3315–3325. <https://doi.org/10.5194/hess-16-3315-2012>
- Sighomnou D (2004) Analyse et redéfinition des régimes climatiques et hydrologiques du Cameroun: perspectives d'évolution des ressources en eau. PhD dissertation, University of Yaounde 1, Yaounde, Cameroon
- Sighomnou D, Descroix L, Genthon P, Mahé G, Moussa BI, Gautier E, Mamadou I, Vandervaere JP, Bachir T, Coulibaly B, Rajot JL, Issa MO, Abdou MM, Dessay N, Delaitre E, Maiga FO, Die-dhiou A, Panthou G, Vischel T, Yacouba H, Karambiri H, Paturel JE, Diello P, Mougou E, Kergoat L, Hiernaux P (2013) The Niger River Niamey flood of 2012: the paroxysm of the Sahelian paradox? *Secheresse* 24:3–13
- Sonkoué D, Monkam D, Fotso-Nguemo TC, Yepdo ZD, Vondou DA (2018) Evaluation and projected changes in daily rainfall characteristics over Central Africa based on a multi-model ensemble mean of CMIP5 simulations. *Theor Appl Climatol*. <https://doi.org/10.1007/s00704-018-2729-5>
- Stanzel P, Kling H, Bauer H (2018) Climate change impact on West African rivers under an ensemble of CORDEX climate projections. *Clim Serv* 11:36–48. <https://doi.org/10.1016/j.clise.r.2018.05.003>
- Tall M, Sylla MB, Diallo I, Pal JS, Faye A, Mbaye ML, Gaye AT (2017) Projected impact of climate change in the hydroclimatology of Senegal with a focus over the Lake of Guiers for the Twenty-first Century. *Theor Appl Climatol* 129(1):655–665. <https://doi.org/10.1007/s00704-016-1805-y>
- Tamoffo AT, Moufouma-Okia W, Dosio A, James R, Pokam WM, Vondou DA, Fotso-Nguemo TC, Guenang GM, Kamsu-Tamo PH, Nikulin G, Longandjo GN, Lennard CJ, Bell JP, Takong RR, Haensler A, Tchotchou LAD, Nouyou R (2019a) Process-oriented assessment of RCA4 regional climate model projections over the Congo Basin under 1.5°C and 2°C global warming levels: influence of regional moisture fluxes. *Clim Dyn* 53(3):1911–1935. <https://doi.org/10.1007/s00382-019-04751-y>
- Tamoffo AT, Vondou DA, Pokam WM, Haensler A, Yepdo ZD, Fotso-Nguemo TC, Tchotchou LAD, Nouyou R (2019b) Daily characteristics of Central African rainfall in the REMO model. *Theor Appl Climatol*. <https://doi.org/10.1007/s00704-018-2745-5>
- Tegegne G, Park DK, Kim YO (2017) Comparison of hydrological models for the assessment of water resources in a data-scarce region, the Upper Blue Nile River Basin. *J Hydrol Reg Stud* 14:49–66. <https://doi.org/10.1016/j.ejrh.2017.10.002>
- Teichmann C, Eggert B, Elizalde A, Haensler A, Jacob D, Kumar P, Moseley C, Pfeifer S, Rechid D, Remedio AR, Ries H, Petersen J, Preuschmann S, Raub T, Saeed F, Sieck K, Weber T (2013) How does a regional climate model modify the projected climate change signal of the driving GCM: a study over different CORDEX regions using REMO. *Atmosphere* 4(2):214–236. <https://doi.org/10.3390/atmos4020214>
- Thomson AM, Calvin KV, Smith SJ, Kyle GP, Volke A, Patel P, Delgado-Arias S, Bond-Lamberty B, Wise MA, Clarke LE, Edmonds JA (2011) RCP4.5: a pathway for stabilization of radiative forcing by 2100. *Clim Change* 109(1):77. <https://doi.org/10.1007/s10584-011-0151-4>
- Thornthwaite CW (1948) An approach towards a rational classification of climate. *Geogr Rev* 38:55–94
- Tiedtke M (1989) A comprehensive mass flux scheme for cumulus parameterization in large-scale models. *Mon Weather Rev* 117(8):1779–1800. [https://doi.org/10.1175/1520-0493\(1989\)117%3C1779:ACMFSF%3E2.0.CO;2](https://doi.org/10.1175/1520-0493(1989)117%3C1779:ACMFSF%3E2.0.CO;2)
- Tomer MD, Schilling KE (2009) A simple approach to distinguish land-use and climate-change effects on watershed hydrology. *J Hydrol* 376:24–33. <https://doi.org/10.1016/j.jhydrol.2009.07.029>
- Tramblay Y, Ruelland D, Somot S, Bouaicha R, Servat E (2013) High-resolution Med-CORDEX regional climate model simulations for hydrological impact studies: a first evaluation of the ALADIN-Climate model in Morocco. *Hydrol Earth Syst Sci* 17:3721–3739
- Tshimanga R, Hughes D (2012) Climate change and impacts on the hydrology of the Congo basin: the case of the northern sub-basins of the Oubangui and Sangha rivers. *Phys Chem Earth, Parts A/B/C* 50–52:72–83. <https://doi.org/10.1016/j.pce.2012.08.002>
- Van Vuuren DP, Stehfest E, den Elzen MGJ, Kram T, van Vliet J, Deetman S, Isaac M, Klein Goldewijk K, Hof A, Mendoza Beltran A, Oostenrijk R, van Ruijven B (2011) RCP2.6: exploring the possibility to keep global mean temperature increase below 2°C. *Clim Change* 109(1):95. <https://doi.org/10.1007/s10584-011-0152-3>
- Vondou DA, Haensler A (2017) Evaluation of simulations with the regional climate model REMO over Central Africa and the effect of increased spatial resolution. *Int J Climatol* 37:741–760. <https://doi.org/10.1002/joc.5035>
- Vörösmarty C, Federer C, Schloss A (1998) Potential evaporation functions compared on us watersheds: possible implications for global-scale water balance and terrestrial ecosystem

- modeling. *J Hydrol* 207(3):147–169. [https://doi.org/10.1016/S0022-1694\(98\)00109-7](https://doi.org/10.1016/S0022-1694(98)00109-7)
- Wu Y, Liu S, Gallant AL (2012) Predicting impacts of increased CO₂ and climate change on the water cycle and water quality in the semiarid James River Basin of the Midwestern USA. *Sci Total Environ* 430:150–160. <https://doi.org/10.1016/j.scitotenv.2012.04.058>
- Xu R, Hu H, Tian F, Li C, Khan MYA (2019) Projected climate change impacts on future streamflow of the Yarlung Tsangpo-Brahmaputra River. *Glob Planet Change* 175:144–159. <https://doi.org/10.1016/j.gloplacha.2019.01.012>
- Yira Y, Diekkrüger B, Steup G, Bossa AY (2017) Impact of climate change on hydrological conditions in a tropical West African catchment using an ensemble of climate simulations. *Hydrol Earth Syst Sci* 21(4):2143–2161. <https://doi.org/10.5194/hess-21-2143-2017>
- Zeilew MB, Alfredsen K (2013) Sensitivity-guided evaluation of the HBV hydrological model parameterization. *J Hydroinform* 15(3):967–990. <https://doi.org/10.2166/hydro.2012.011>

Publisher's Note Springer Nature remains neutral with regard to jurisdictional claims in published maps and institutional affiliations.